Mechanics Research Communications 116 (2021) 103764

Contents lists available at ScienceDirect

Mechanics Research Communications

journal homepage: www.elsevier.com/locate/mechrescom

Uncertainty of pipe flow friction factor equations

Luiz Eduardo Muzzo [a], Gláucio Kenji Matoba [a], Luís Frölén Ribeiro [a,b,*]

[a] Instituto Politécnico de Bragança, Campus de Santa Apolónia, Bragança, 5300-253, Portugal
[b] LAETA – INEGI, Campus da FEUP, Porto, 4200-465, Portugal

ARTICLE INFO

MSC:
0000
1111

Keywords:
Friction factor
Fluid flow
Colebrook equation

ABSTRACT

This paper presents the turbulent pipe flow analysis of the friction factor's uncertainty for two different experimental scenarios: high-precision and standard engineering instruments. One deduced the uncertainty function of the implicit Colebrook's correlation and five of the most accurate and fast explicit correlations. The joint propagation of uncertainties is evaluated, sorted and mapped for the probabilities of intersection of the Colebrook's uncertainties against the alternative correlations. The maps display the fastest to the slowest equation for standard engineering and high-precision instruments, respectively for 50% and 95% intersection. For the standard engineering instruments, the least accurate of the explicit correlations are applicable and within the Colebrook uncertainty bounds. The most accurate correlations are necessary for specific roughness and Reynolds'o domains cases and for high-precision research instruments. Results also show that, for high-precision scenarios with a 95% uncertainty fit, there is still room for improvement in the explicit correlations.

1. Introduction and objectives

In pipe flows, the head loss depletes mechanical energy from the fluid flow due to friction from both viscosity and surface roughness. This friction is quantified by the friction factor and is calculated analytically for laminar flows. For turbulent flows, one may calculate it two ways: by solving the implicit equation defined by Colebrook's works; by solving explicit equations that have been appearing in the literature since then. Colebrook [1] presented Eq. (1) for the friction factor in commercial pipes:

$$\frac{1}{\sqrt{f}} = -2\log_{10}\left(\frac{\epsilon/D}{3.7} + \frac{2.51}{\mathrm{Re}\sqrt{f}}\right) \tag{1}$$

where f is the friction factor, ϵ/D is the relative roughness, ϵ is the equivalent sand-grain roughness, D is the hydraulic diameter of the pipe, Re is the Reynolds number. The Colebrook equation is based on experimental data from earlier works by Prandtl, von Kármán and Nikuradse [2]. It is the accepted standard for friction factor calculation, although not in total agreement with recent experimental measurements, neither in terms of values nor terms of curve behavior in the region of transition from smooth to rough hydraulic regimes [3,4].

The importance of the works from Colebrook is undeniable as it sets the benchmark. To ease daily engineering practice, in 1944, Moody plotted his famous chart for the friction factor in commercial pipes using this equation for the turbulent regime on the range of $0 \leq \epsilon/D \leq 0.05$ by $3000 \leq \mathrm{Re} \leq 1 \times 10^8$ [5]. As computers and respective software become more complex, the computational burden to calculate the implicit equation (1) for every branch of fluid pipe network increases. Consequently, many explicit correlations were developed to mitigate the burden of the friction factor calculation. From an evaluation of the published research, from Moody himself in 1947 to the most recent publications offering new explicit correlations [6–8], one may conclude that the search for the best explicit correlation has not yet ended.

As these explicit correlations are approximations to Colebrook's, previous proposals balanced the analysis of the trade-off between accuracy and time. The accuracy is always compared against results from the Colebrook equation [9–12]. Computational time is the final result of a complex set of variables where the complexity of the model, the numerical approach, and hardware may play an important goal to improve the velocity of calculation of the friction factor.

Alternative approaches such as applying genetic optimization [13] or the application of asymptotic series expansion of the Wright and Lambert ω-function and symbolic regression [8,14] are relevant from a mathematical and computational standpoint. Despite the high-precision approximations, the friction factor calculation for real pipe networks always depends on measured values being thus susceptible to their intrinsic uncertainties as pointed out by [15] that modeled the uncertainty functions of the Colebrook quantities applying the Monte

* Corresponding author at: Instituto Politécnico de Bragança, Campus de Santa Apolónia, Bragança, 5300-253, Portugal.
E-mail address: frolen@ipb.pt (L. Frölén Ribeiro).

https://doi.org/10.1016/j.mechrescom.2021.103764
Received 10 March 2021; Received in revised form 2 August 2021; Accepted 9 August 2021
Available online 15 August 2021

Carlo method. Still, the implicit Colebrook correlation as a benchmark exempt from experimental uncertainties is rooted in these previous works.

This work aims to evaluate the uncertainty propagation of the most accurate explicit correlations for the friction factor and verify if their high-accuracy is relevant when the uncertainties of the experimental quantities are included. The — How accurate is accurate enough? — question is the trigger of this work, which may be expanded into the following three questions:

1. How important is it to obtain an exact match for the friction coefficient when incorporating the instrument precision?
2. May a strategy to select the best-suited correlations, including the instrument precision, be proposed?
3. Is it worth it to improve the already very accurate explicit correlations when the experimental uncertainty is far larger, as it will be demonstrated in this article?

2. Theory and methods

2.1. Current explicit correlations

An exhaustive review of explicit correlations since the seminal work by Colebrook is presented by [16]. It presents the average and maximum relative errors of the explicit correlations against Colebrook's and the computational time, and the best trade-off between accuracy and computing burden is depicted in a 2-D diagram for 30 correlations. The five correlations with the best balance between computational time and accuracy, ordered here from the fastest to the slowest, and less accurate to most accurate, were found to be:

1. Eq. (2) by Haaland [17], which differs with less than ±1.5% against the Colebrook equation, is the fastest correlation among the recommended ones. All equations on this list have the same application range as the Colebrook equation: $0 \le \epsilon/D \le 0.05$ by $3000 \le \mathrm{Re} \le 1 \times 10^8$.

$$f = \left\{ -1.8 \log_{10} \left[\frac{6,9}{\mathrm{Re}} + \left(\frac{\epsilon/D}{3.7} \right)^{1.11} \right] \right\}^{-2} \tag{2}$$

2. Eq. (3) by Fang et al. [18], with maximum relative error of 0.50% compared with the Colebrook equation:

$$f = 1.613 \left\{ ln \left[0.234 \left(\frac{\epsilon}{D} \right)^{1.1007} - \frac{60.525}{\mathrm{Re}^{1.1105}} + \frac{56.291}{\mathrm{Re}^{1.0712}} \right] \right\}^{-2} \tag{3}$$

3. Eqs. (4), (5), (6) and (7) by Brkić and Praks [7], with which the Colebrook equation is in balance with a relative error of no more than 0.13%:

$$f = \left[0.8686 \left(A_1 - C_1 + \frac{C_1}{A_1 + B_1} \right) \right]^{-2} \tag{4}$$

$$A_1 = \ln \mathrm{Re} - 0.779397488 \tag{5}$$

$$B_1 = \frac{\mathrm{Re}\,(\epsilon/D)}{8.0878} \tag{6}$$

$$C_1 = \ln\left(A_1 + B_1\right) \tag{7}$$

4. Eqs. (8) and (9) by Shacham [19], which correlates the correct solution of the Colebrook equation within 0.02% relative error.

$$f = \left\{ \left[A_2(1 - \ln A_2) - \frac{\epsilon/D}{3.7} \right] \Big/ \left(1.15129 A_2 + \frac{2.51}{\mathrm{Re}} \right) \right\}^{-2} \tag{8}$$

$$A_2 = \frac{\epsilon/D}{3.7} - \frac{5.02}{\mathrm{Re}} \log_{10} \left(\frac{\epsilon/D}{3.7} + \frac{14.5}{\mathrm{Re}} \right) \tag{9}$$

5. Eqs. (10), (11), (12) and (13) by Serghides [20]. This correlation is the most accurate one, with a maximum relative error of 0.00314%. Although it is the slowest explicit correlation, it consumes less than half of the time required in the iterative calculation of Colebrook's equation [16].

$$f = \left[A_3 - \frac{(B_3 - A_3)^2}{A_3 - 2B_3 + C_3} \right]^{-2} \tag{10}$$

$$A_3 = -2 \log_{10} \left(\frac{\epsilon/D}{3.7} + \frac{12}{\mathrm{Re}} \right) \tag{11}$$

$$B_3 = -2 \log_{10} \left(\frac{\epsilon/D}{3.7} + \frac{2.51 A_3}{\mathrm{Re}} \right) \tag{12}$$

$$C_3 = -2 \log_{10} \left(\frac{\epsilon/D}{3.7} + \frac{2.51 B_3}{\mathrm{Re}} \right) \tag{13}$$

2.2. Measurement uncertainties

The friction factor is a function of roughness and Reynolds. Thus it depends on measured values of diameter, surface roughness, flow velocity/rate and fluid properties. Accuracy, calibration, and operating procedures of instrumentation, the operator's skill, pipe roundness, and fluid temperature may propagate uncertainties to the friction factor.

Common instruments for measuring inner pipe diameter are calipers and tape/laser measures. The uncertainty of high-precision calipers range from ±0.02 mm to ±0.04 mm (±0.0008 in to ±0.0016 in) while standard instruments range from ±0.05 mm to ±0.1 mm (±0.002 in to ±0.004 in) [21]. Pipes with half-inch diameter can be measured within an uncertainty of less than ±0.8%, for instance, and this percentage is lowered for larger diameters. Tape/laser measures cover the range of larger diameters, when it is impractical to use calipers, and achieve accuracies of ±1 mm to ±3 mm (±0.04 in to ±0.12 in). These instruments are sufficiently accurate for fluid flow applications, but thermal expansion or ovality may further increase the uncertainty associated with the pipe's diameter.

Flowmeters, such as differential pressure, positive displacement, and ultrasonic meters have accuracy ranging from ±0.25% to ±10% [22]. Viscosity is measured by viscometers with accuracies ranging from ±0.2% to ±5% of full scale, but common fluids like water and air have their properties tabulated. Although varied sources present slightly different values, the largest viscosity uncertainty is due to fluid temperature uncertainty. For example, the kinematic viscosity of water is $1.01 \times 10^{-6}\ \mathrm{m^2\,s^{-1}}$ ($1.09 \times 10^{-3}\ \mathrm{ft^2\,s^{-1}}$) at 293.15 K (68 °F) [23], but for temperatures 5 K (9 °F) higher the viscosity decreases 11.3%, and for temperatures 5 K lower, it increases 12.9%.

Roughness is the largest source of uncertainty. In the experiments that led to Colebrook's equation, the pipe's roughness was artificially made with sand-grains. Therefore, the roughness of the pipe ought to be an equivalent sand-grain roughness. Recommended values for commercial ducts of various materials are, for example, tabulated in [24], with uncertainties up to ±70%. Alternatively, using the roughness parameter Rz, the calculated friction factor value differs on average 6.75% from experimental results [25]. Rz is the arithmetic average of the maximum peak to valley heights within five sampling lengths and can be measured by roughness testers, which achieve accuracies from ±0.5% to ±5%.

2.3. Uncertainty propagation analysis

When a measured value is used to calculate another, the former's measurement uncertainties are propagated to the latter. The uncertainty propagation is given by Eq. (14) [26]:

$$\Omega_F = \sqrt{\sum_{i=1}^{n} \left(\frac{\partial F}{\partial m_i} \Omega_{m_i} \right)^2} \tag{14}$$

where Ω_F is the absolute uncertainty of the calculated value F and Ω_{m_i}, of the measured value m_i. Eq. (15) is rearranged in terms of relative (percentage) uncertainty ω.

$$\omega_F = \sqrt{\sum_{i=1}^{n} \left(\frac{\partial F}{\partial m_i} \frac{m_i}{F} \omega_{m_i} \right)^2} \tag{15}$$

The friction factor functions in four quantities: roughness, diameter, flow velocity and kinematic viscosity. Therefore, its relative uncertainty may be given by Eq. (16).

$$\omega_f = \left[\left(\frac{\partial f}{\partial \epsilon} \frac{\epsilon}{f} \omega_\epsilon \right)^2 + \left(\frac{\partial f}{\partial u} \frac{u}{f} \omega_u \right)^2 + \left(\frac{\partial f}{\partial D} \frac{D}{f} \omega_D \right)^2 + \left(\frac{\partial f}{\partial \nu} \frac{\nu}{f} \omega_\nu \right)^2 \right]^{1/2} \tag{16}$$

Eq. (16) can be simplified into Eq. (17), where the uncertainty of the friction factor is a function of relative roughness and Reynolds.

$$\omega_f = \left[\left(\frac{\partial f}{\partial (\epsilon/D)} \frac{\epsilon/D}{f} \omega_{(\epsilon/D)} \right)^2 + \left(\frac{\partial f}{\partial \mathrm{Re}} \frac{\mathrm{Re}}{f} \omega_{\mathrm{Re}} \right)^2 \right]^{1/2} \tag{17}$$

Thus, friction factor uncertainty ω_f is a function of the uncertainties of roughness, $\omega_{(\epsilon/D)}$, and of Reynolds, ω_{Re}. They are given by Eqs. (18) and (19) as functions of the uncertainties of: surface roughness ω_ϵ, diameter ω_D, flow velocity ω_u and kinematic viscosity ω_ν.

$$\omega_{(\epsilon/D)} = \sqrt{{\omega_\epsilon}^2 + {\omega_D}^2} \tag{18}$$

$$\omega_{\mathrm{Re}} = \sqrt{{\omega_u}^2 + {\omega_D}^2 + {\omega_\nu}^2} \tag{19}$$

3. Results and discussion

3.1. Uncertainty of the friction factor — Colebrook

The uncertainty of the friction factor calculation with Eq. (17) is completed once the weight coefficients given by Eq. (20) and (21) are know.

$$W_{(\epsilon/D)} = \left| \frac{\partial f}{\partial (\epsilon/D)} \frac{\epsilon/D}{f} \right| \tag{20}$$

$$W_{\mathrm{Re}} = \left| \frac{\partial f}{\partial \mathrm{Re}} \frac{\mathrm{Re}}{f} \right| \tag{21}$$

The weight parameters are functions of roughness and Reynolds and are depicted in Figs. 1(a) and 1(b) within the range of $1 \times 10^{-7} \leq \epsilon/D \leq 0.05$ by $3000 \leq \mathrm{Re} \leq 1 \times 10^8$. These calculations were carried out for the Colebrook equation (1) expanded to 12 iterations of the method of successive substitution. Curve behavior and values are similar for explicit correlations.

For low relative roughness, i.e. smoother pipes, and low Reynolds, the influence of roughness uncertainty is negligible when compared to Reynolds's. Also, it is independent of the roughness value. This is expected since the friction factor is less dependent on roughness when this is small and more dependent on Reynolds when the effect of viscous friction is more relevant (low Re). The largest weight value of the uncertainty of Reynolds is 0.307 for the smallest roughness and Reynolds. The dashed line is the frontier were both weight coefficients from Eqs. (20) and (21) have the same value. For high roughness and Reynolds, the uncertainty of roughness becomes dominant. Its influence is the largest for the highest roughness and Reynolds: 0.465. The weight of relative roughness tends to be unconstrained by the Reynolds number. This region is characterized as hydraulic rough since the energy loss due to surface roughness is more relevant when compared to that due to the effect of viscosity. Figs. 1(a) and 1(b) is useful to decide which instruments need to be accurate depending on the application's hydraulic regime.

The friction factor uncertainty is calculated for two representative scenarios: high-precision research and standard engineering instruments. For high-precision research, where accurate instruments and measurement protocols are mandatory, the following experimental uncertainties are assumed: 3% for surface roughness; 0.1% for diameter; 0.5% for flow velocity; 0.5% for kinematic viscosity. For engineering projects, the assumed uncertainties are roughness 60%; diameter 2%; flow velocity 10%; viscosity 10%.

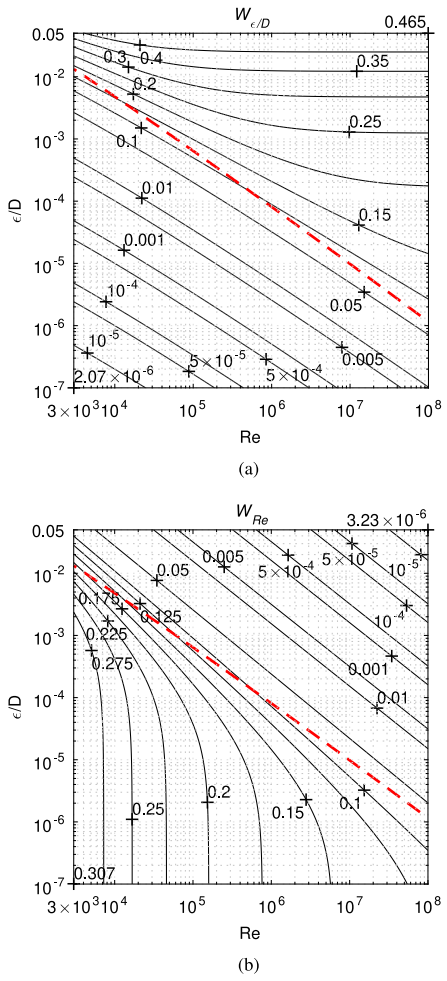

Fig. 1. (a) Weights of relative roughness uncertainty, Eq. (20), and (b) Reynolds number uncertainty, Eq. (21), in the friction factor's uncertainty calculated from Eq. (17). The dashed line (red) shows the border were both weights have the same value and delimits the region where the uncertainty of Reynolds is dominant (lower region) from the one where roughness is more relevant (upper region).

The relative uncertainty of the friction factor calculated for the Colebrook equation is depicted in Fig. 2 for standard (utmost y-axis) and high-precision scenarios (left y-axis). For high-precision instruments, the friction factor uncertainty is between 0.07% and 1.40%, while for the engineering case, the final uncertainty can be as high as 28.00%. Notably, the instrumental uncertainties for the standard engineering scenario are 20 times larger than the values of ω_ϵ, ω_D, ω_u and ω_ν for the high-precision research scenario, and this reflects into 20 times larger ω_f. Another feature in Fig. 2 is that the larger the relative roughness, the larger the uncertainty of the friction factor. Reynolds influence friction factor uncertainty in smoother pipes and less turbulent flow, and roughness dominates in rougher pipes and more turbulent regimes. This behavior agrees with that shown in Figs. 1(a) and 1(b).

The friction factor calculated from the implicit Colebrook equation is presented in Fig. 3 by a circle. The respective uncertainty range for the standard measurement scenario marks the possible limits of the friction factor results. The results of the five explicit correlations are depicted with dots displaying the high fit of all explicit correlations. Visually they appear falling inside the same single dot, but a carefully

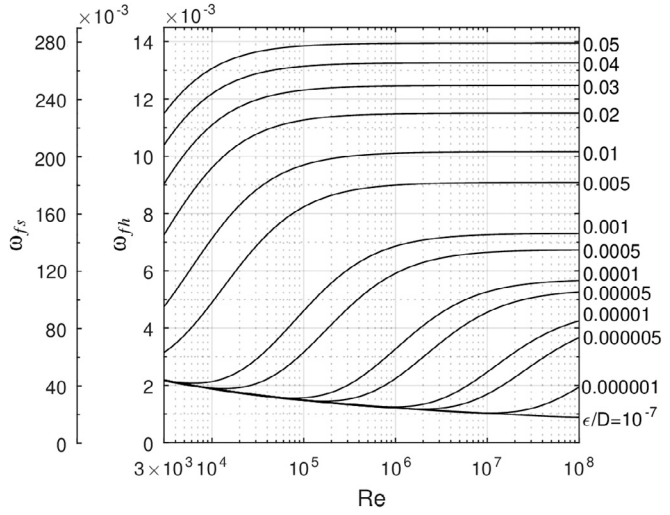

Fig. 2. Friction factor relative (percentage) uncertainty for standard and high-precision scenarios, ω_{fs} and ω_{fh}.

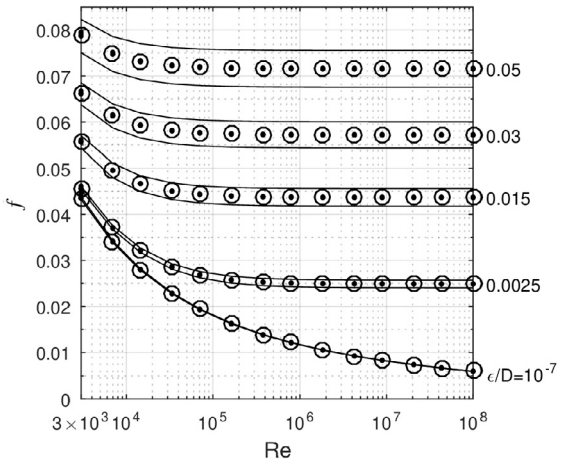

Fig. 3. Colebrook's and the five explicit correlations' friction factors (respectively circles and dots) with the uncertainty limits for standard engineering scenario.

visual enlargement shows that not to be the case. This could be enough to justify that all correlations inside the Colebrook equation's uncertainty range are perfectly viable for friction calculation, but their own propagated uncertainties should also be tested. Again, the larger the friction factor, f, the wider the uncertainty limits for all correlations.

3.2. Uncertainty of the friction factor — Explicit correlations

The uncertainty of each explicit correlation is compared against Colebrook's owns uncertainty. The possible arrangements of the uncertainty adjustments are depicted in Figs. 4(a) to 4(f). The concurrence is evaluated by the ratio of the intersected area by possible total, defined by the non-dimensional fitness τ parameter (probability of intersection), Eq. (22), where f_1 and f_2 are respectively the upper lines of correlation 1 and 2 while f_3 and f_4 are respectively the lower lines, Fig. 4(b). In the cases where there is no intersection the fitness is zeroed, Fig. 4(a).

$$\tau = \frac{f_2 - f_3}{f_1 - f_4} \tag{22}$$

Figs. 4(a) to 4(f) depict the different scenarios for the intersection of the uncertainty limits of the functions. The continuous lines represent

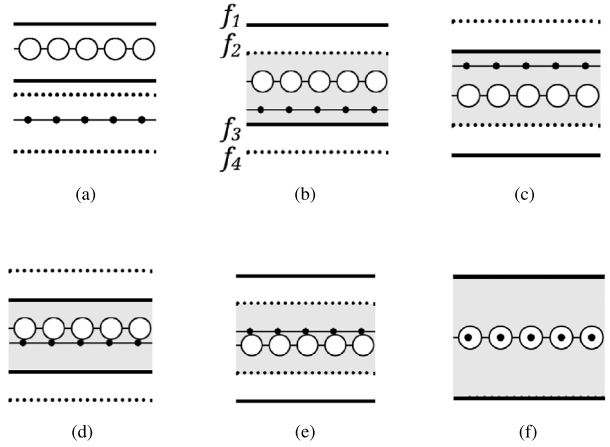

Fig. 4. Intersection area between the uncertainty ranges of the Colebrook correlation (circles), limited by continuous lines, and an explicit correlation (dots), limited by dotted lines.

the Colebrook uncertainty limits, and the dotted lines the uncertainty limits of any other correlation. The first case is the no-interference between the uncertainty limits for $\tau = 0$, Fig. 4(a). The opposite limit is the exact fit of the uncertainty limits of both functions for $\tau = 1$, Fig. 4(f). The true value of the friction factor may be at any point between these extremes for combinations in Figs. 4(b) to 4(e). In Fig. 4(b), the uncertainty limit of Colebrook expression is partially overlaid (shadowed area) by the explicit correlation in the lower part of the schema. As for Fig. 4(c), the superposition is in the upper part of the schema. In these two situations, the uncertainty limits of both functions are equally spaced. Figs. 4(d) and 4(e) are for situations where the uncertainty limits are different. In the first one, Colebrook's uncertainty limits are narrower than the explicit function - Fig. 4(d). The opposite case is when Colebrook's uncertainty limits are wider than the explicit function - Fig. 4(e).

The true value of the friction factor may be located at any point between the limits of uncertainty. Presumably, it will be inside the area delimited by the Colebrook equation (admitting it is the most reality-accurate equation, although the inconsistencies with some experimental results [3,4]). The larger the fitness parameter, or the shadowed areas in Figs. 4(b) to 4(f), the larger the probability that the calculated friction factor will fall inside Colebrook's uncertainty limits by using that particular explicit correlation.

The fitness parameter is used as a quantitative criterion to compare different explicit equations. To illustrate, one will describe the methodology for everyday engineering instruments and $\tau \geq 0.950$. Fig. 5(a) shows that the Serghides correlation, Eqs. (10) to (13), satisfies the criteria for all domain. Nevertheless, a faster but slightly less accurate correlation as Shacham, Eqs. (8) and (9) also perform correctly for the same fitness and replaces Serghides almost all over the domain, overlaying the previous areas with the faster Shacham correlations. Fig. 5(b) shows the areas satisfied by the fastest correlations that comply with the fitness parameter, where the green layer from Shacham tops the red layer from Serghides correlation. The only part that it does not cover is where $\tau < 0.950$. Brkić and Praks and Fang correlations successively decrease the computational burden, thus overlaying the previous slower equations in Figs. 5(c) and 5(d). The final diagrams of the fastest explicit equations to the fitness of 95% are concluded when Haaland correlation is the last to be superimposed with the yellow shading, Fig. 6(a).

Figs. 6(a) and 6(b) depict respectively the standard engineering and high-precision scenarios for all correlations evaluated in this article, for $\tau \geq 0.950$. Fig. 6(a) shows that the Shacham correlation is the most suitable for smaller roughness and Reynolds; and that the correlations

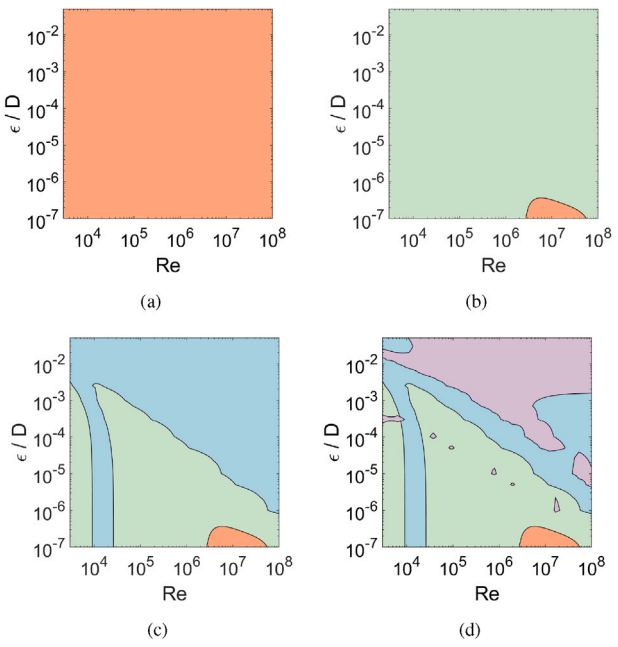

Fig. 5. Trustful values in the intersection area, for $\tau \geq 95\%$. Graphics from (a) to (d) show the overlays of the correlation for standard precision instruments. Serghides (red), Shacham (green), Brkić and Praks (blue) and Fang (purple). (For interpretation of the references to color in this figure legend, the reader is referred to the web version of this article.)

from Brkić and Praks, Fang et al. and Haaland dominate the upper region of larger roughness and Reynolds. By reducing the fitness criteria to $\tau \geq 0.785$, Brkić and Praks correlation, Eqs. (4) to (7), will cover the whole domain, and by further reducing to $\tau \geq 0.252$, Fang et al. Eq. (3), will also suffice. Haaland's correlation does not satisfy the whole domain for any value of τ different than zero.

For high-precision scenario and fitness 95%, equations by Serghides and Shacham are the fastest that cover the domain partially, Fig. 6(b). The blank area indicates that none of the explicit correlation satisfies the Colebrook correlation for $\tau \geq 0.950$ for that area. Although, if one reduces the fitness value to $\tau \geq 0.840$, the Serghides correlation will cover the whole domain, and if further reduced to $\tau \geq 0.270$, Shacham correlation will also suffice. In the high-precision scenario, correlations by Haaland, by Fang et al. and by Brkić and Praks do not cover the whole domain for any value of τ.

The reduction of fitness does not imply necessarily a decrease in accuracy. The uncertainty values are much smaller for lower Re and roughness, Figs. 2 and 3, and thus the probability of intersection may decrease. By setting the fitness parameter to $\tau \geq 50\%$, one may observe in Figs. 7(a) and 7(b) the recommended correlation domain maps, respectively, for standard engineering and high-precision instruments. For the first, Brkić and Praks, Serghides, and Shacham explicit correlations cover the whole domain. However, there is no needed to use these higher precision correlations because Haaland and Fang et al. correlations, Eqs. (2) and (3), present faster results with the same degree of uncertainty. Correlation by Haaland is recommended when roughness and Reynolds are larger, and the lower diagonal region of Fig. 7(a) is occupied by correlations from Fang et al. and Brkić and Praks.

Fig. 7(b) shows a similar trend as Fig. 6(a). Haaland region is smaller, and only for limited values of Re and ϵ/D is applicable. Fang et al. region is quite similar; this correlation is recommended for high values of $1 \times 10^5 \leq \text{Re} \leq 1 \times 10^8$ and $3 \times 10^{-3} \leq \epsilon/D \leq 0.05$. Brkić and Praks region is similar to Fig. 6(a), and it covers the upper half of the domain.

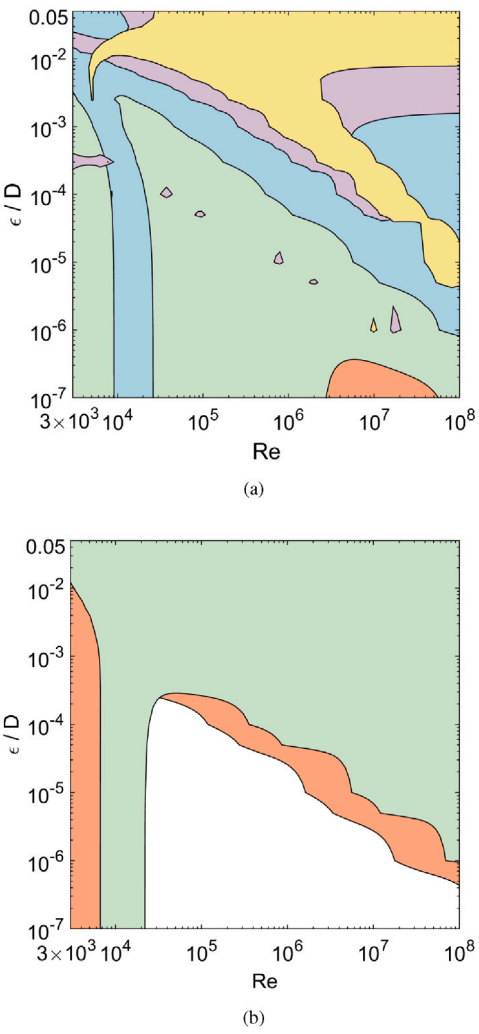

Fig. 6. Trustful values in the intersection area, for $\tau \geq 95\%$. (a) Standard precision instruments and (b) high-precision instruments. Serghides (red), Shacham (green), Brkić and Praks (blue), Fang et al. (purple) and Haaland (yellow). (For interpretation of the references to color in this figure legend, the reader is referred to the web version of this article.)

4. Conclusions

The early work of Colebrook was experimental, and experimental uncertainty depends on the type of approach: standard or high-precision. How important it is to obtain an exact match for the friction coefficient when incorporating the instrument precision was recognized with the assessment of experimental uncertainty for this schema. For the standard practices, long-established correlations such as Fang et al.'s or Halaand's more than suffice. There is still room for improvement for high-precision experiments when the goal is to reach a close-to-exact match between Colebrook's and explicit correlations.

This paper presents a strategy based on a fitness parameter proposed to quantify the propagated uncertainty analysis of both the implicit and explicit correlations in calculating the friction factor in circular pipes flow. The fitness factor τ parameterizes the intersection between the uncertainties of the Colebrook and the explicit equations. This parameter allows sorting the probability of the intersection of uncertainties of the correlations in Reynolds' roughness domain. The results are mapped for 2 types of probability, 95%, and 50%, and standard and high-precision instruments, Figs. 6 and 7. Fair to state that when correlations yield a result with the same degree of uncertainty and differ only in

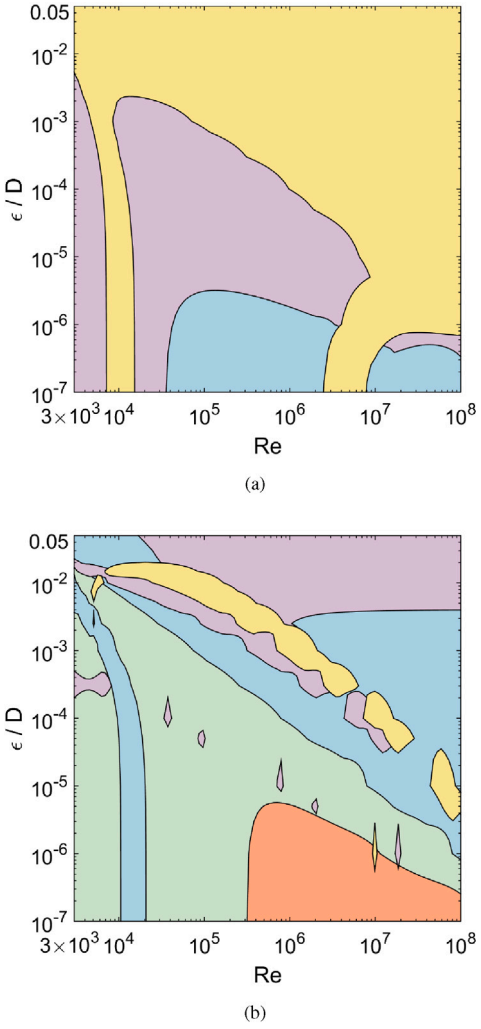

Fig. 7. Trustful values in the intersection area, for $\tau \geq 50\%$. (a) Standard precision instruments and (b) high-precision instruments. Serghides (red), Shacham (green), Brkić and Praks (blue), Fang et al. (purple) and Haaland (yellow). (For interpretation of the references to color in this figure legend, the reader is referred to the web version of this article.)

complexity and computing time, it is futile to use the most intricate or time-consuming.

Fig. 6(b), the high-precision scenario with a 95% probability of intersection, will allow us to return the last question — Is it worth it to improve the already very accurate explicit correlations when the experimental uncertainty is far more considerable? — The use of high-precision equipment decreases uncertainty, thus reduces the probability of intersection. There is a void in Fig. 6(b) showing that none of the evaluated equations comply with the criteria. However, relaxing the criteria from the original 95% to 84% fitness enables Serghides correlation over the whole domain. As the fitness parameter is relaxed, the choices of valid equations broader, Fig. 7(b).

An unexpected consequence of the uncertainty analysis is comparing the relative roughness and Reynolds weights that will enable the selection of suitable instruments according to the domain conditions, Figs. 1(a) and 1(b).

Declaration of competing interest

The authors declare that they have no known competing financial interests or personal relationships that could have appeared to influence the work reported in this paper.

Funding

This work was funded by national funds through FCT - Fundação para a Ciência e Tecnologia, through project UIDB/50022/2020 - LAETA.

References

[1] C.F. Colebrook, Turbulent flow in pipes, with particular reference to the transition region between the smooth and rough pipe laws, J. Inst. Civ. Eng. 11 (4) (1939) 133–156.
[2] C.F. Colebrook, C.M. White, Experiments with fluid friction in roughened pipes, Proc. R. Soc. A 161 (906) (1937) 367–381.
[3] M.A. Shockling, J.J. Allen, A.J. Smits, Roughness effects in turbulent pipe flow, J. Fluid Mech. 564 (2006) 267–285.
[4] L.I. Langelandsvik, G.J. Kunkel, A.J. Smits, Flow in a commercial steel pipe, J. Fluid Mech. 595 (2008) 323–339.
[5] L.F. Moody, Friction factors for pipe flow, Trans. ASME 66 (1944) 671–684.
[6] L.F. Moody, An approximate formula for pipe friction factors, Trans. Am. Soc. Mech. Eng. 69 (12) (1947) 1005–1011.
[7] D. Brkić, P. Praks, Accurate and efficient explicit approximations of the Colebrook flow friction equation based on the Wright ω-function, Mathematics 7 (1) (2019) 34.
[8] P. Praks, D. Brkić, Review of new flow friction equations: Constructing Colebrook's explicit correlations accurately, Rev. Internac. Métod. Numér. Cálc. Diseñ. Ingr. A 36 (2020) http://dx.doi.org/10.23967/j.rimni.2020.09.001.
[9] G. Yildirim, Computer-based analysis of explicit approximations to the implicit Colebrook–White equation in turbulent flow friction factor calculation, Adv. Eng. Softw. 40 (11) (2009) 1183–1190.
[10] D. Brkić, Review of explicit approximations to the Colebrook relation for flow friction, J. Pet. Sci. Eng. 77 (1) (2011) 34–48.
[11] S. Genić, I. Arandjelović, P. Kolendić, M. Jarić, N. Budimir, V. Genić, A review of explicit approximations of Colebrook's equation, FME Trans. 39 (2) (2011) 67–71.
[12] H.K. Winning, T. Coole, Explicit friction factor accuracy and computational efficiency for turbulent flow in pipes, Flow Turbul. Combust. 90 (1) (2013) 1–27.
[13] D. Brkić, Ž. Ćojbašić, Evolutionary optimization of Colebrook's turbulent flow friction approximations, Fluids 2 (2) (2017).
[14] D. Brkić, Z. Stajić, Excel vba-based user defined functions for highly precise colebrook's pipe flow friction approximations: a comparative overview, Facta Universit. Ser.: Mech. Engrg. (2021).
[15] I. Lira, On the uncertainties stemming from use of the Colebrook-White equation, Ind. Eng. Chem. Res. 52 (22) (2013) 7550–7555, http://dx.doi.org/10.1021/ie4001053.
[16] L.E. Muzzo, D. Pinho, L.E.M. Lima, L.F. Ribeiro, Accuracy/speed analysis of pipe friction factor correlations, in: Proceedings of the 2nd International Congress on Engineering and Sustainability in the XXI Century, Springer Nature Switzerland AG, 2019, pp. 664–679.
[17] S.E. Haaland, Simple and explicit formulas for the friction factor in turbulent pipe flow, J. Fluids Eng. 105 (1) (1983) 89–90.
[18] X. Fang, Y. Xu, Z. Zhou, New correlations of single-phase friction factor for turbulent pipe flow and evaluation of existing single-phase friction factor correlations, Nucl. Eng. Des. 241 (3) (2011) 897–902.
[19] M. Shacham, Comments on: "An explicit equation for friction factor in pipe", Ind. Eng. Chem. Fundam. 19 (2) (1980) 228.
[20] T.K. Serghides, Estimate friction factor accurately, Chem. Eng. 91 (1984) 63–64.
[21] F.T. Farago, M.A. Curtis, Handbook of Dimensional Measurement, Industrial Press Inc., 1994.
[22] P.J. LaNasa, E.L. Upp, Fluid Flow Measurement: A Practical Guide to Accurate Flow Measurement, Butterworth-Heinemann, 2014.
[23] P.J. Pritchard, J.W. Mitchell, Fox and McDonald's Introduction to Fluid Mechanics, John Wiley & Sons, 2011.
[24] F.M. White, Fluid Mechanics, McGraw-Hill, 2011.
[25] F.F. Farshad, H.H. Rieke, Flow Test Validation of Direct Measurement Methods Used to Determine Surface Roughness in Pipes (OCTG), Society of Petroleum Engineers Inc., 2002.
[26] J.P. Holman, Experimental Methods for Engineers, McGraw-Hill, 2012.